Microstructure, strength and tribological behavior of Fe–C–Cu–Ni sintered steels prepared with MoS$_2$ addition

S. Dhanasekaran · R. Gnanamoorthy

Abstract Powder metal processing permits development of new composites with specific properties required for demanding applications. Complex shaped machine elements like gears and bearings are made of powder metallurgy technique economically. In many applications these machine elements operate under unlubricated conditions and there is a need for materials with good friction and wear characteristics, strength and modulus. In the present study, Fe–C–Cu–Ni alloys with solid lubricant, MoS$_2$, were developed using a simple single stage compaction and sintering. The microstructure, strength, hardness and tribo behavior of the composites were evaluated. The friction and wear characteristics were evaluated using pin-on-disc type tribo test machine. Addition of solid lubricant improved the compressibility and thereby the density of the compacts. Presence of the secondary sulphide phases in the as-sintered compacts improves the hardness and strength. The coefficient of friction and wear loss decreased with addition of MoS$_2$. A simple wear model is proposed to predict the wear loss in these composites. The model predicts wear loss values that are in agreement with the experimental data.

Introduction

Sintered steels with various alloying additions have been developed for an increasing number of applications such as gears, connecting rods, bearings etc., Powder metal (P/M) processing permits development of new material compositions for applications which require a combination of properties. For applications involving the sliding, rolling and rolling/sliding contact high strength, high hardness, low coefficient of friction, and good wear resistance are the important requirements. Various elements are added to sintered steels to improve the compressibility, hardness, strength, machinability and toughness [1]. Sintered steels for heavy duty applications, in general, contain copper, nickel, molybdenum and chromium. Good dimensional control was obtained with the addition of nickel and copper. Copper melts during sintering and together with nickel control the physical properties [2]. In recent years, sintered steels with hard sulphides, carbides, nitrides and fluorides were developed which exhibit high strength and good tribological properties [3, 4]. Bronze, iron and nickel powder composites containing fullerene like WS$_2$ nanoparticles are developed by Rapoport et al. [3]. Impregnation of WS$_2$ particles in pores improves the tribological behavior. Addition of TiC was found to improve the strength and wear resistance of high speed steels [4]. Wear resistance of the high speed steels containing MnS, CaF$_2$ and TiC was studied by Zuomin et al. [5]. The TiC addition was found to enhance the wear resistance while the additions MnS and CaF$_2$ do not improve the wear resistance but improve the self lubricating properties [5].

Sintered materials have inherent porosity and the presence of pores have both beneficial and detrimental role on the part performance. Pores act as stress concentration zones and reduce the mechanical strength. Porosity reduces the effective cross sectional area and increases the amount of stress transferred

S. Dhanasekaran · R. Gnanamoorthy (✉)
Department of Mechanical Engineering, Indian Institute of Technology Madras, Chennai 600 036, India
e-mail: gmoorthy@iitm.ac.in

across the material bridges between the pores. Increase in density increases the strength, fracture toughness and resistance to crack growth [6]. The contact fatigue behavior of sintered steels was also significantly influenced by the material composition and density [7, 8]. Cracks were found initiated below the contact surface under pure rolling conditions and propagate towards the surface [8]. Presence of pores affects the endurance limit strength under rolling contact fatigue conditions. The strength of a material is inversely proportional to the cross sectional area of the pores [9]. The material wear under dry sliding conditions depends upon material composition, normal load, sliding velocity and surface conditions. Sintering temperature and sintering atmosphere affects the microstructure and density and was found to influence the wear characteristics of sintered steels [10]. Different wear mechanisms such as adhesive, oxidation and abrasive are possible in the sintered steels. The applied stresses, sliding velocity and surface morphology, in addition to the material composition and processing conditions decides the nature of wear.

Gears and bearings, in many applications, operate under dry conditions. Different alloying additions and surface treatments are employed to reduce the friction and wear characteristics. Alloying with lead, manganese, etc., was found to improve both the machinability and tribo characteristics. An attempt is made to develop Fe–C–Cu–Ni sintered steels with solid lubricant, MoS_2. Microstructure, strength and hardness of the developed materials are reported. The friction and wear characteristics under dry sliding conditions were discussed.

Test materials and experimental details

Test materials, processing and characterization

Test compositions with the nominal compositions mentioned in Table 1 were prepared from the elemental powders. The iron powder particle size was balanced –150 to +45 μm. The detail of iron powder is mentioned in Table 2. Carbon, copper and nickel

Table 2 Designation and specifications of iron powder

Designations	ASI 100.29 (Atomized iron powders)
H_2O Loss	0.01%
Carbon	<0.01%
Sulphur	0.01%
Flow rate	27 s/50 gms
Apparent density	2.95 g/cm^3
Green density	7.1 g/cm^3
Powder size	–150 to +45 μm—Balance

powders finer grades (<50 μm) were used. MoS_2 powder of size ~10 μm was added to the base compositions. The weighed powders were mixed using a double cone mixture and the mixing time was 30 min. Zinc stearate was used as die lubricant. The alloy powders were compacted into cylindrical specimens of 10 mm diameter and 15 mm length using a hydraulic press at room temperature. The compaction pressure employed was 500 MPa. The green compact was sintered at 1393 K (1120 °C) under 90% N_2 + 10% H_2 atmosphere for 30 min. The density and inter connected porosity were measured according to the ASTM standards [11]. The microstructure and pore morphology were studied on the metallographically prepared samples using optical and scanning electron microscopes.

Hardness of metallographically prepared samples was measured using a Vickers hardness tester at an applied load of 5 kg. Hardness measurements were performed at different places on the surface of polished specimen. At least six measurements were taken on each sample and the mean values are used. Compression tests were carried out using a universal testing machine. Cylindrical specimens of 10 mm diameter and 15 mm length are used for measuring the compression strength. The length to diameter ratio is less then two and is normally used to avoid buckling [12, 13].

Friction and wear test details

Sliding wear tests were carried out using a pin-on-disc tribometer under dry sliding conditions. All test

Table 1 Hardness, strength, density and porosity of test materials

| Nominal Composition	Hardness (Hv)	Compressive strength (N/mm^2)	Density (g/cm^3)	Interconnected porosity (%)
Fe–0.6%C–2.5%Cu–3%Ni	93 ± 1	535 ± 8	6.35 ± 0.02	10.0 ± 0.2
Fe–0.6%C–2.5%Cu–3%Ni–3%MoS_2	137 ± 2	1184 ± 12	6.51 ± 0.03	4.7 ± 0.1
Fe–0.6%C–2.5%Cu–3%Ni–5%MoS_2	159 ± 1	1273 ± 12	6.70 ± 0.02	4.2 ± 0.1

Table 3 Chemical composition of disc material (wt. %)

C	Mn	Si	P	S	Ni	Cr
0.90–1.10	1.10 max	0.10–0.35	0.05 max	0.05 max	Nil	1.00–1.50

specimens were mated against the hardened alloy steel, AISI 52100. The chemical composition of disc material is mentioned in Table 3. The AISI 52100 disc was heat treated at a temperature of 1118 K (845 °C) followed by oil quenching and tempering at 423 K (150 °C) for 1 h to attain the hardness of 60 ± 2 HRc. Prior to testing the disc was ground and polished and the centerline average surface roughness was 0.12 μm. The disc was cleaned in acetone using an ultrasonic cleaning machine before wear tests. The details of pin-on-disc wear test rig are described elsewhere [14]. Sintered cylindrical pins were machined to a diameter of 5 mm up to a length of 8 mm. The initial surface roughness was measured using the diamond tipped profilometer at three places. The initial weight of pins was measured using an electronic weighing balance with 0.1 mg accuracy after cleaning in acetone followed by drying. The sliding wear tests were performed at a constant velocity of 0.3 m s^{-1} and up to a sliding distance of 4000 m. Tests were conducted at different normal loads, 5, 10, 15 and 20 N. The wear loss was determined as the change in weight of sintered steel pin measured before and after the test. At least three tests were conducted at each condition and the results were averaged. The friction force was continuously measured using a load cell. The wear rate was evaluated from the volume of worn out material divided by the sliding distance. The volume of worn out material was evaluated from the weight loss divided by the density of material. The worn surfaces of pins were observed using optical and scanning electron microscope.

Results and discussion

Density, microstructure, hardness and strength

The density and interconnected porosity measured according to ASTM standards [11] are given in Table 1. Addition of MoS$_2$ increased the sintered part density and decreased the porosity. Presence of solid lubricant powders during compaction increases the compressibility and improves the density. Similar results were reported by Sustarsic et al. [15] in vacuum sintered stainless steel compositions containing MoS$_2$.
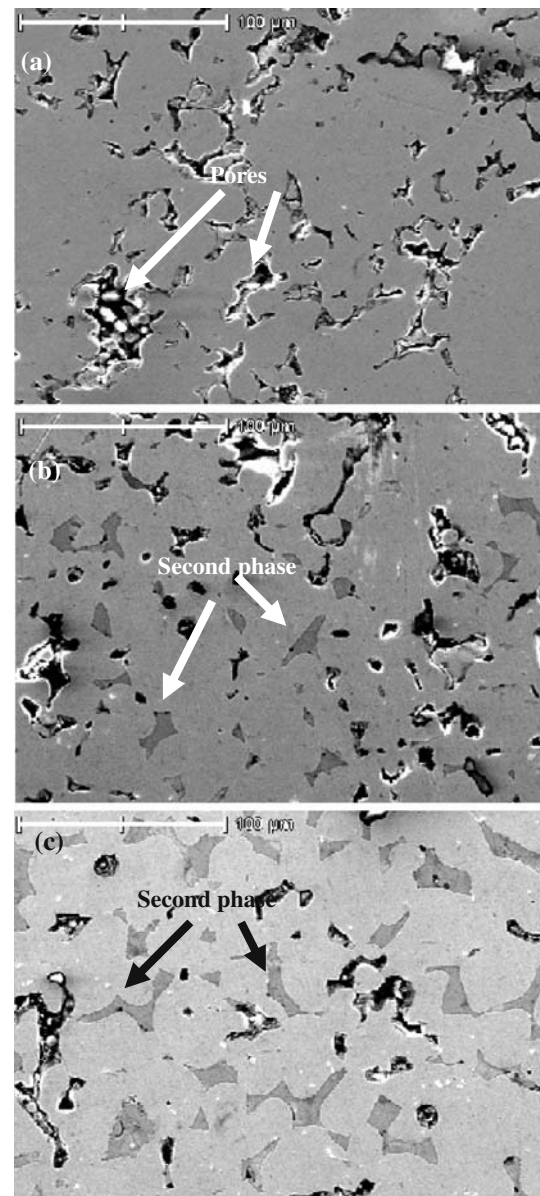
Fig. 1 Scanning electron micrograph showing the pore morphology and second phase in test materials (**a**) Fe–C–Cu–Ni (**b**) Fe–C–Cu–Ni–3%MoS$_2$ and (**c**) Fe–C–Cu–Ni–5%MoS$_2$

The microstructure of test materials is shown in Fig. 1. A large number of pores were observed in base composition, Fe–C–Cu–Ni, indicating the low density. Addition of the nickel has no influence on the densification and pore morphology of as-sintered products and microstructure are similar to that of the Fe–C–Cu composition [16]. The microstructure of MoS$_2$ added samples indicate a less number of pores compared with the base composition and the size of pore is also small [Fig. 1]. The micrographs also show the presence of second phase grey color regions which were not observed in the base composition. The second

phases are approximately few tens of microns in size and are irregularly shaped. The volume fraction of second phases was measured using an image analyzer. The volume fraction is about 4.6% and 9% for the 3% and 5% MoS_2 added compositions respectively. A higher volume fraction of second sulphide phases were observed in materials containing higher content of MoS_2. The detail EDS section analysis conducted indicate the presence of S and Mo in the second phases in addition to the weak Cu peak. No Fe or Ni was detected in the second phase. This indicates the decomposition of MoS_2 during sintering leading to formation of complex sulphides [17]. However, detail analysis is required for identification of second phase formed. The studies conducted by Danninger et al. [18] also indicate the decomposition of admixed solid lubricants during sintering in iron–carbon system. The second phases hereafter are referred as secondary sulphide phases.

The hardness and compressive strength of test materials are given in Table 1. The increase in the part density and presence of hard sulphide phases contribute to the increase in the hardness of MoS_2 added samples. The hardness and strength of the nickel added Fe–Cu–C sintered steels [16] are higher than that of the Fe–C–Cu composition indicating the solid solution hardening due to addition of nickel. Presence of more volume fraction of hard sulphide phases

increases the hardness of MoS_2 added samples. The Fe–C–Cu–Ni + 5% MoS_2 alloy exhibited a highest hardness of about 160 HV and compressive strength of about 1293 MPa in the as-sintered condition due to presence of higher volume fraction of hard sulphide phases and increased part density. The improved strength and reduction in ductility due to the presence of high volume fraction of hard secondary phases causes cracking in high 5% MoS_2 added composition.

Coefficient of friction

The variations of coefficient of friction of sintered steels when slide against hardened AISI 52100 steel at a normal load of 10 and 20 N are shown in Fig. 2. The initial coefficient of friction was lower for the MoS_2 added samples compared to base composition. The friction coefficient rises in a short time in all the test materials indicating the breaking of oxide layer present in the material. The friction coefficient which varies during the initial period stabilizes after 500 m of sliding. This period is referred as the run-in period and is more or less same for all the materials investigated. The maximum coefficient of friction during the run-in period is high for the base composition and decreases with increase in MoS_2 composition. The nature of oxide layer composition formed depends on the base composition and decides the

Fig. 2 Variation of friction coefficient for the test materials at normal loads (a) 10 N and (b) 20 N
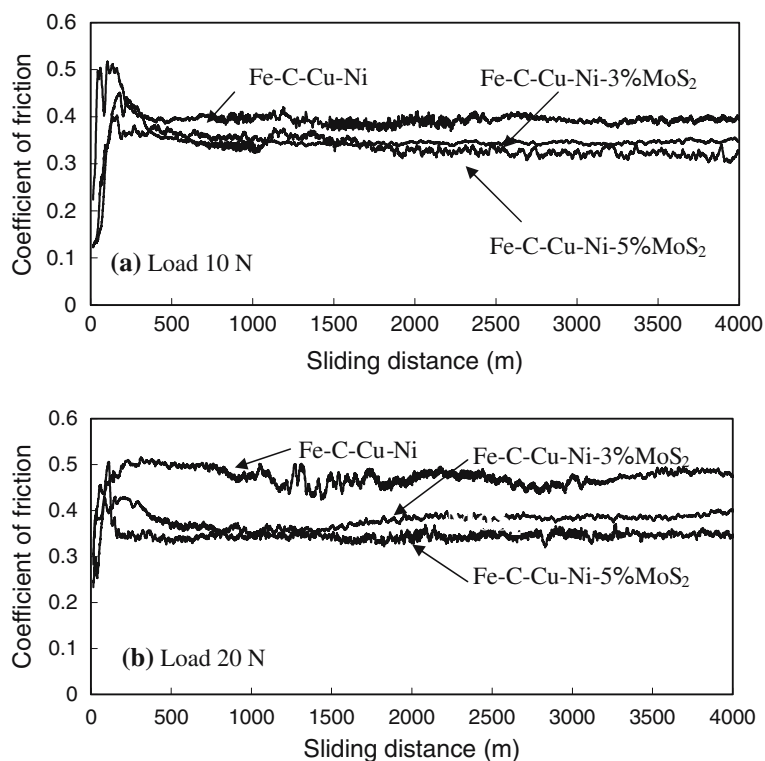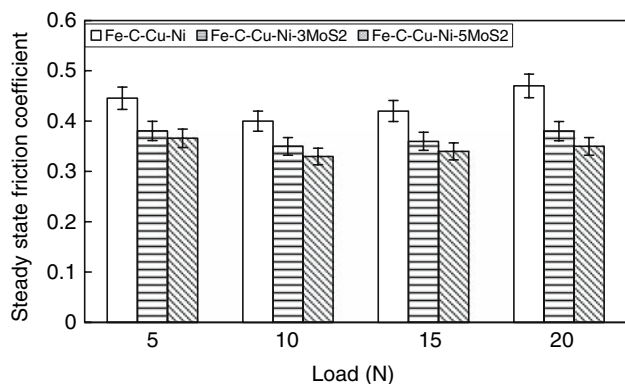
Fig. 3 Steady state friction coefficients at different normal loads for test materials

Fig. 4 Wear rate of test samples at different normal loads

Fig. 5 Wear coefficient of test samples at different normal loads

magnitude of coefficient of friction. With further sliding as the metal-to-metal contact occurs the coefficient of friction reduces and reaches a steady state.

At high applied normal loads, the shear stresses exceed the material shear strength, and cause severe plastic deformation. The second phase particles present near the surface are liberated first during the sliding process and serves as a solid lubricant. The sulphide particles present below the surface are released due to the continuous sliding wear process and maintain a constant steady state coefficient of friction with a less variation in the friction coefficient. Figure 3 shows the steady state friction coefficient at different normal loads for all the test materials. The steady state coefficient of friction is nearly constant at all applied normal loads in a material. Presence of lubricating hard sulphide particles plays a significant role in reducing the friction coefficient at all normal loads investigated. Materials containing high volume of second phase exhibited a lower coefficient of friction. It has been reported that the WS_2 particles present in the sintered alloys were gradually transferred to the metal surfaces during sliding and reduced friction coefficient [19].

Wear loss

The wear rates of sintered steel compositions at different normal loads were evaluated based on the mass loss measurements carried out before and after the sliding tests. Figure 4 shows the wear rate of test materials at different normal loads investigated. The wear rate increases with increasing applied normal load for all the test materials and addition of MoS_2 improved the wear resistance of Fe–C–Cu–Ni alloys. The low wear rates in the MoS_2 added materials can be attributed to the presence of hard sulphide lubricating phase and increased density. Higher amount of second
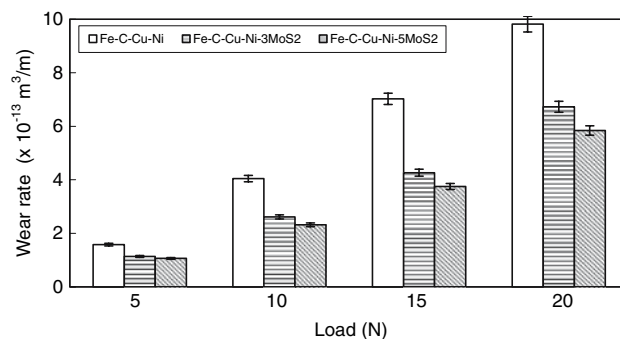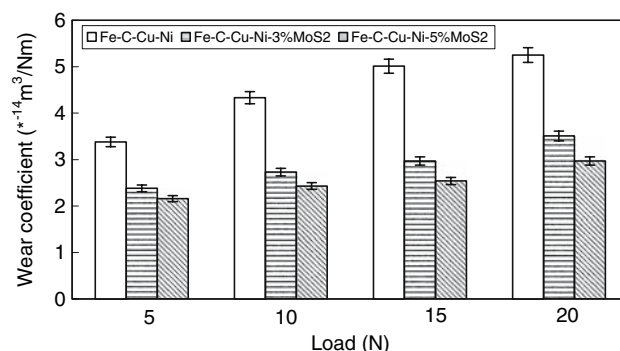
phases in 5 % MoS_2 added composition resulted in the lower wear rate, 5.85×10^{-13} m^3 / m. Presence of pores decreases the hardness, strength and fracture toughness of sintered steels [20]. The low hardness and fracture toughness of low density base composition reduces the wear resistance. Figure 5 illustrates the effect of composition on the wear coefficient. The MoS_2 containing samples have better response then the base composition. The porosity is detrimental in the base composition which increases the wear coefficient. The wear coefficient is low in MoS_2 containing samples. In the materials investigated there is a good correlation between the hardness and the wear resistance. Figure 6 shows the mass loss of the material at all normal load plotted against the hardness. Materials with higher harness exhibited a lower mass loss.
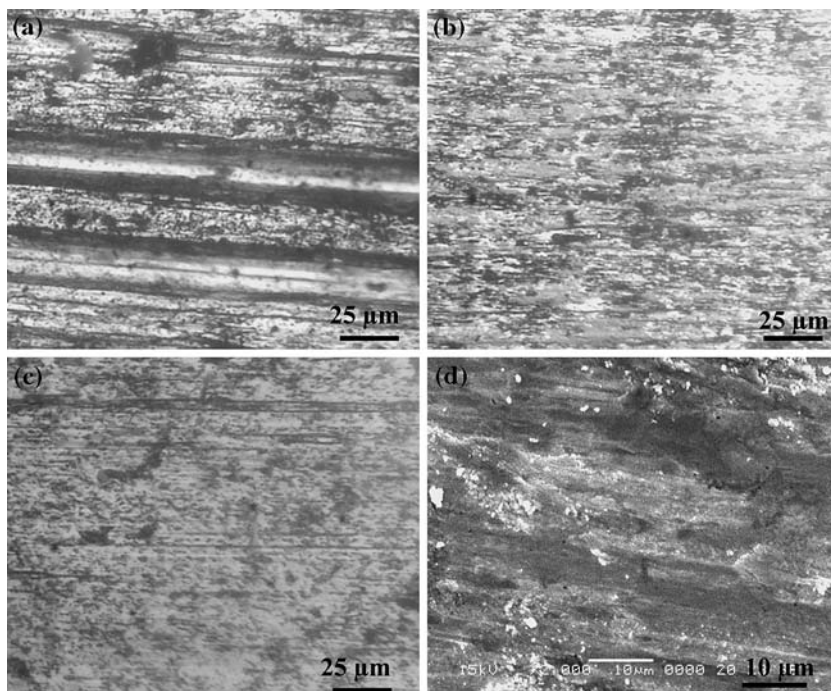
Wear mechanism

Different wear mechanisms contribute to wear of porous composites. Distinct features were observed on the worn surfaces and depend upon the material composition. A very rough wear surface with deeper wear tracks were observed in the base material indicating higher coefficient of friction and severe material wear loss (Fig. 7a).
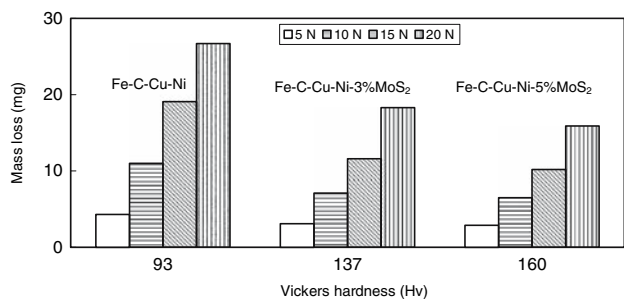
Fig. 6 Mass loss versus hardness of the test material under sliding conditions

Presence of pores increases the stress concentration around the pores and act as generation sites of wear. The material deformation occurs near the pores leading the breakage of particles. In specimens containing MoS_2 the wear tracks were not as distinct as that in the base composition (Figs. 7b and c). Relatively smoother worn surfaces were observed in the MoS_2 added compositions indicating the lubricating effect of the secondary sulphide phase. The worn out surface also show the thin film of sheared particles on the surfaces indicating the lubricant film formation by the second phase which was not observed in the base composition. These dark smooth surfaces when viewed under scanning electron micrograph in the MoS_2 added samples contribute to a low coefficient of friction (Fig. 7d). The pores visible are smaller and fewer number in MoS_2 added composition due to the increased part density.

Wear model

The wear of porous composites is very complex. The material loss occurs during sliding due to adhesive, oxidative and abrasive wear mechanisms. A wear model based on the approaches followed by Srivastava et al. [21] and Zhang et al. [22] is proposed for the sintered composites. It is assumed that the well known Archard wear equation describes the wear process of materials investigated. The fundamental Archard wear equation is
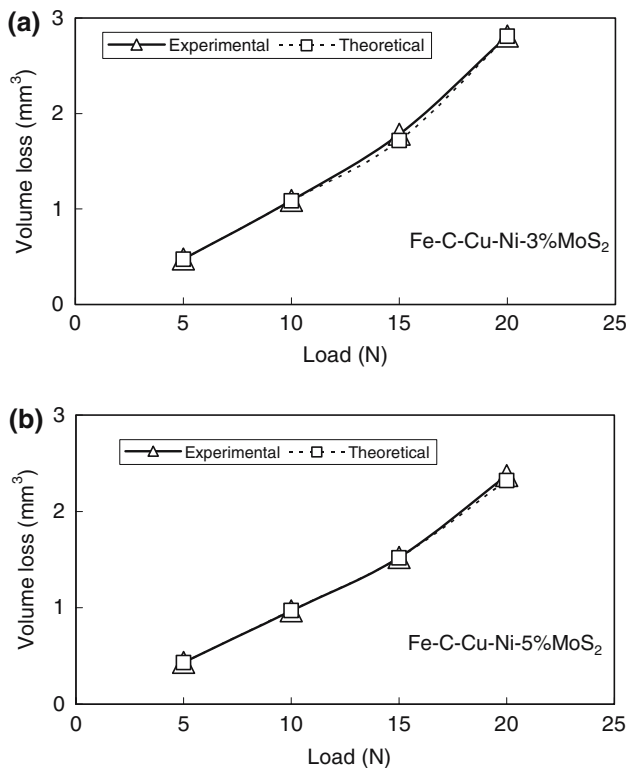
$$V = K_1 \frac{PL}{H} \tag{1}$$

where V is the volumetric wear of sintered steel pin, L is the sliding distance, K_1 is the wear coefficient, H is the hardness of sintered steel pin and P is the applied normal load. The differential equation which governs the adhesive wear process as a function of applied normal load is

$$\frac{dV}{dP} = K_1 \frac{L}{H} + K_2 V \tag{2}$$

Here K_2 is a constant related to the probability of particle removal and the second term in the right hand side of this equation refers the volume of wear increase with respect to increment of load.

$$K_2 = K_3 \frac{f_v}{d(1 - f_v)} \tag{3}$$

Fig. 7 Worn surfaces of the (**a**) Fe–C–Cu–Ni (**b**) Fe–C–Cu–Ni–3%MoS$_2$ (**c**) Fe–C–Cu–Ni–5%MoS$_2$ and (**d**) Fe–C–Cu–Ni–5%MoS$_2$ (SEM)

Fig. 8 Predicted and experimental wear volumes for the composite materials investigated

Here f_v is the volume fraction of secondary sulphide phase present in the composition and d is the size of second phase particles which is about 10 μm.

Integration of Eq. 2 yields

$$V = C_1 e^{K_2 P} - \frac{K_1 L}{K_2 H} \qquad (4)$$

where C_1 is a constant. Initially $P = 0$ and $V = 0$, therefore, $C_1 = \frac{K_1 L}{K_2 H}$

The wear volume of sintered steel pin at any load P is therefore

$$V = \frac{K_1}{K_3} \frac{L}{H} \frac{(1 - f_v)d}{f_v} \left[e^{\frac{K_3 f_v P}{d(1 - f_v)}} - 1 \right] \qquad (5)$$

The wear volume of composite material depends on the amount of second phase, applied load, and hardness. The values K_1 and K_2 in the above equation are determined from experimental results which take care of the effect of porosity inherent to powder metal processed materials. The predicted wear volume using the above model along with experimental results under different load conditions for the MoS_2 added compositions are shown in Fig. 8. The predicted values are in

good agreement with the experimentally measured wear volumes for the MoS_2 added compositions with the error less than 5%. The experimental and theoretical results show that volume loss of the sintered steel pin increases with increasing applied normal load, and decreases with increasing sulphide content.

Conclusions

The Fe–C–Cu–Ni + MoS_2 composites were prepared using powder metallurgy processing route exhibited high density. The addition of MoS_2 improves the compressibility and increases the part density. The volume fraction of secondary sulphide phases formed depends on the MoS_2 addition and decides the hardness and compressive strength. Materials with 5% MoS_2 exhibited highest hardness and strength. The coefficient of friction when slide against hardened and ground wrought steel disc is low for the composites. Thin layer of sulphide phase forms a lubricating film on the mating surface and reduces the friction coefficient. The wear resistance of the base alloys was also improved due to addition of MoS_2. The proposed wear model for the composites predicts the wear volumes which are in close agreement with the experimental results.

References

1. Rapport L, Leshchinsky V, Lvovsky M, Lapsker I, Volovik YU, Tenne R (2002) Tribology Int 35:47
2. Danninger H (1993) Powder Metal Sci Tech 4:22
3. Rapoport L, Leshchinsky V, Lvovsky M, Nepomnyashchy O, Volovik YU, Tenne R (2002) Wear 252:518
4. Velasco F, Gordo E, Isabel R, Ruiz Navas EM, Bautista A, Torralba JM (2001) Int J Refractory Metals Hard Mater 19:319
5. Zuomin L, Childs THC (2004) Wear 257:435
6. Fleck NA, Smith RA (1981) Powder Metal 3:121
7. Gnanamoorthy R, Rajiv N, Gopinath K, Miyashita Y, Mutoh Y (2002) ASM Int J Practical Failure Anal 2:71
8. Gnanamoorthy R, Govindarajan N, Mutoh Y (2004) ASM J Failure Anal Prevention 4:78
9. Kubicki B (1995) Powder Metal 38:295
10. Wang J, Danninger H (1998) Wear 222:49
11. ASTM B 328 (1996) Standard test method for density, oil content and interconnected porosity of sintered metal structural parts and oil-impregnated bearings, ASTM International, West Conshohocken, p 108
12. Howard A. Kuhn (1999) ASM Hand book **11** p 143
13. ASTM E 9-89 a, ''Standard test methods of compression testing of metallic materials at room temperature'', (ASTM International, West Conshohocken, 2000) p 104

14. Srinath G, Gnanamoorthy R (2005) J Mater Sci 40:2897
15. Sustarsic B, Kosec L, Jenko M, Leskovsek V (2001) Vacuum 61:471
16. Dhanasekaran S, Gnanamoorthy R (2007) Mater Design 28:1135
17. Dhanasekaran S, Gnanamoorthy R, Unpublished results
18. Danninger H, Liersch A, Ratzi R (2000) In: Kosuge K, Nagai H (eds) Proceedings of 2000 powder metallurgy world congress, (2000, Japan Powder Metallurgy Association) p 1108
19. Rapoport L, Lvovsky M, Lapsker I, Leshchinsky W, Volovik Yu, Feldman Y, Tenne R (2001) Wear 249:150
20. Candela N, Velasco F, JM Torralba (1999) Mater Sci Eng A 259:98
21. Srivastava AK, Sriram K, Lal GK (1988) Int J Mach Tool Manufact 28:181
22. Zhang Z, Zhang L, Mai YW (1996) Wear 194:38